applied sciences

MDPI

Article

Fluorene–Triphenylamine-Based Bipolar Materials: Fluorescent Emitter and Host for Yellow Phosphorescent OLEDs

Ramanaskanda Braveenth [1], Hasu Jung [1], Keunhwa Kim [1], Bo Mi Kim [2], Il-Ji Bae [3], Miyoung Kim [3,*] and Kyu Yun Chai [1,*]

1 Division of Bio-Nanochemistry, College of Natural Sciences, Wonkwang University, Iksan 570-749, Korea; braveenth.czbt@gmail.com (R.B.); junghs1117@naver.com (H.J.); qeutesl@naver.com (K.K.)
2 Department of Chemical Engineering, Wonkwang University, Iksan 570-749, Korea; 123456@wku.ac.kr
3 Nano-Convergence Research Center, Korea Electronics Technology Institute, Jeonju 54853, Korea; ijbae@keti.re.kr
* Correspondence: miy1kim@keti.re.kr (M.K.); geuyoon@wonkwang.ac.kr (K.Y.C.); Tel.: +82-632-190-011 (M.K.); +82-638-506-230 (K.Y.C.)

Received: 27 November 2019; Accepted: 7 January 2020; Published: 10 January 2020

Abstract: In this study, two new bipolar materials were designed and synthesized: N^1-(9,9-diphenyl-9*H*-fluoren-2-yl)-N^1-(4,6-diphenylpyrimidin-2-yl)-N^4,N^4-diphenylbenzene-1,4-diamine (FLU-TPA/PYR) and N^1-(4-(4,6-diphenyl-1,3,5-triazin-2-yl)phenyl)-N^1-(9,9-diphenyl-9*H*-fluoren-2-yl)-N^4,N^4 diphenylbenzene-1,4-diamine (FLU-TPA/TRZ). We fabricated two different devices, namely a yellow phosphorescent organic light-emitting diode (PhOLED) and a non-doped fluorescent OLED emitter with both FLU-TPA/PYR and FLU-TPA/TRZ. The FLU-TPA/PYR host-based yellow PhOLED device showed better maximum current, power and external quantum efficiencies at 21.70 cd/A, 13.64 lm/W and 7.75%, respectively. The observed efficiencies were better than those of the triazine-based FLU-TPA/TRZ. The non-doped fluorescent device with the triazine-based FLU-TPA/TRZ material demonstrated current, power and external quantum efficiencies of 10.30 cd/A, 6.47 lm/W and 3.57%, respectively.

Keywords: organic light-emitting diodes; fluorene; host material; triazine; pyrimidine

1. Introduction

Organic light-emitting diodes (OLEDs) have become an interesting component in research and commercial markets. OLEDs show prominent advantages over traditional displays, namely their high contrast, high brightness, wide view angle, lack of back light requirements, light weight and thin films. OLEDs continue to be used for next-generation displays in mobile phones, televisions and other lighting resources, where they help to reduce the energy consumption [1–6].

First-generation OLEDs are known as fluorescence OLEDs, and these were able to contribute only 25% of internal quantum efficiency while losing 75% in a non-radiative manner [7–9]. Later, phosphorescent OLEDs with metal and ligand complexes were identified as second-generation emitters in OLEDs. Within these, iridium and platinum-based heavy metal complexes were utilized to obtain triplet and singlet energies, and they showed an achievable internal quantum efficiency of 100% [10–15]. Such maximal internal quantum efficiency was able to be reach through the intersystem crossing mechanism (ISC). This process requires the heavy metal-based phosphorescent emitter to be doped with a suitable host material with an appropriate doping concentration [16–24]. This helps to reduce the quenching process, such as aggregation-caused quenching (ACQ) and triplet–triplet annihilation (TTA) [25–29]. Third-generation OLEDs are metal-free fluorescent emitters that use suitable donor

and acceptor molecules as building blocks. These type of emitters are known as thermally activated delayed fluorescence (TADF) emitters, and they work based on the reverse intersystem crossing (RISC) mechanism [30–34]. Both phosphorescent and TADF OLEDs need an efficient host material to enhance device efficiencies [35,36].

There are three types of host materials that have been reported, namely hole transport (HT) type, electron transport (ET) type, and bipolar host materials. HT type host materials are made of electron-donating triphenylamine, carbazole and acridine derivatives. 4,4′-bis(*N*-carbazolyl)-1,1′-biphenyl (CBP), 1,3-bis(*N*-carbazolyl)benzene (mCP), and 4,4′-cyclohexyli denebis[*N*,*N*-bis(4-methylphenyl)benzenamine] (TAPC) are well-known HT type host materials, but they do not show stable thermal properties. Tris(8-hydroxyquinoline)aluminum (Alq_3) and Bis[2-(diphenylphosphino)phenyl] ether oxide (DPEPO) are ET type host materials that are used in phosphorescent and TADF OLEDs [37–49]. Host materials are essential energy suppliers to the dopant material that also prevent energy flow back from the dopant. Host materials should possess a higher triplet energy than that of the dopant material. At the same time, host materials should have suitable frontier molecular orbital energies (FMOs) to ensure effective carrier transportation from the adjacent layers [50–52].

Bipolar host materials have received much attention from research communities due to their bipolar nature. Bipolar host materials contain electron-donating and electron-accepting units in a single molecule. Moreover, bipolar host materials can provide proper carrier balance while supporting an effective carrier recombination at the emission layer [53–57]. Mostly, bipolar materials can be utilized for host materials as well as fluorescent emitters. In the present study, we designed and synthesized two new types of bipolar materials, namely N^1-(9,9-diphenyl-9*H*-fluoren-2-yl)-N^1-(4,6-diphenylpyrimidin-2-yl)-N^4,N^4-diphenylbenzene-1,4-diami ne (FLU-TPA/PYR) and N^1-(4-(4,6-diphenyl-1,3,5-triazin-2-yl)phenyl)-N^1-(9,9-diphenyl-9*H*-fluoren-2-yl) -N^4,N^4 diphenylbenzene-1,4-diamine (FLU-TPA/TRZ). These two new materials have an N^1-(9,9-diphenyl-9*H*-fluoren-2-yl)-N^4,N^4-diphenylbenzene-1,4-diamine donor and a triazine or pyrimidine acceptor incorporated into them. They were used as a yellow host and as a non-doped fluorescence emitter. Iridium(III) bis(4-(4-*tert*-butylphenyl) thieno[3,2-c]pyridinato-*N*,C2′) acetylacetonate (PO-O1) was employed as a yellow phosphorescent dopant.

2. Materials and Methods

2.1. Materials

2-amino-9,9-diphenylfluorene (**1**), 2-(4-Bromophenyl)-4,6-diphenyl-1,3,5-triazine (**7**), 2-Chloro-4,6-diphenyl-1,3,5-triazine (**6**) and 4-Iodotriphenylamine (**2**) were obtained from TCI chemicals (Seoul Korea). $Pd(OAc)_2$, $Pd(PPh_3)_4$ and NaO*t*Bu were purchased from Sigma-Aldrich (Seoul, Korea). Toluene, dichloromethane, *n*-hexane and ethyl acetate were obtained from SK chemicals (Seongnam-si, Gyeonggi-do, Korea). Toluene was distilled from sodium/benzophenone before use. Analytical thin layer chromatography (TLC) was conducted by using an aluminum-backed Merck Kieselgel 60 coated TLC plate with visualizations of 254 and 365 nm (Seoul, Korea). Column chromatography was performed with silica gel (mesh size of 200–300). Reverse osmosis (RO) water was used for all purposes related to this work.

2.2. Instrumentation

^{1}H and ^{13}C NMR analyses were performed with a JEON JNM-ECP FT-NMR spectrometer (Peabody, MA, USA) operating at 500 MHz. The UV–Vis absorbance property was analyzed with a Lambda 1050 ultraviolet visible (UV–VIS) spectrophotometer (Perkin Elmer, Waltham, MA, USA). The energy of the band gap (Eg) was obtained from the onset wavelength of the UV–Vis absorbance spectra. Photoluminescence (PL) spectra were measured with an HR800 spectrofluorometer (Horiba Jobin Yvon, Paris, France). Mass spectrometry analysis was carried out with a Xevo TQ-S spectrometer (Waters,

Milford, MA, USA). An elemental analysis (EA) was performed with a ThermoFisher (Flash 2000) elemental analyzer (Loughborough, England). Thermal gravimetric analysis (TGA) and differential scanning calorimetry (DSC) were recorded with a PerkinElmer DSC 4000 and TGA 8000 system (Melville, NY, USA) under a nitrogen atmosphere with a heating rate of 10 °C/min. The triplet energy level (ET) was estimated from the onset wavelength of the emission spectra at 77 K in toluene. The HOMO (highest occupied molecular orbital) value was determined by a AC-2 method with a photoelectron spectrometer (RIKEN, Saitama, Japan). The LUMO (lowest unoccupied molecular orbital) energy was calculated by adding the band gap energy to the obtained HOMO energy. OLED devices were constructed with a thermal evaporating system under a pressure of 5×10^{-7} torr (Sunicel plus, Seoul, Korea). Current density–voltage–luminescence (*J–V–L*) performances were observed by an OLED *I–V–L* test system (Polarmix M6100, Suwon, Korea). The electroluminescence (EL) spectra were recorded with a spectroradiometer (Konica Minolta CS-2000, Tokyo, Japan).

2.3. Synthesis of N^1-(9,9-diphenyl-9H-fluoren-2-yl)-N^4,N^4-diphenylbenzene-1,4-diamine (3)

A mixture of 9,9-diphenyl-9*H*-fluoren-2-amine (1, 1.0 g, 2.99 mmol), 4-iodo-*N*,*N*-diphenylaniline (2, 1.22 g, 3.29 mmol), palladium (II) acetate ($Pd(OAc)_2$, 0.1 g, 0.45 mmol), sodium *tert*-butoxide (NaO*t*Bu, 0.43 g, 4.49 mmol), 10% tri-*tert*-butylphosphine in toluene (tBu_3P, 0.20 mL, 0.89 mmol) and anhydrous toluene (80 mL) was added into a two-neck round-bottom flask that was equipped with a condenser. The above mixture was subjected to a vacuum, and then a nitrogen atmosphere was provided. The mixture was refluxed at 110 °C for 10 h while being stirred with a magnetic bar. After the completion of the reaction, a crude mixture was made up by using dichloromethane (250 mL) and deionized water (125 mL) three times. The organic layer was collected and dried over anhydrous magnesium sulphate. After filtration, the crude mixture was evaporated by using a rotary evaporator. The target molecule (3) was achieved via silica column chromatography with an *n*-hexane:dichloromethane (2:1) solvent system (Scheme 1).

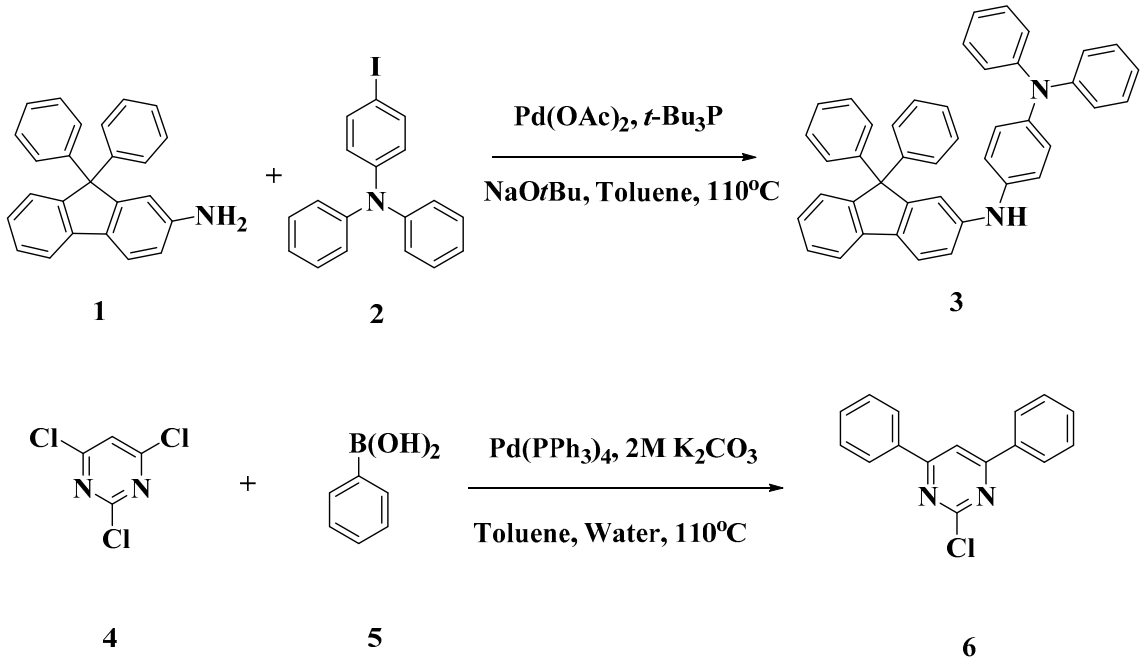

Scheme 1. Synthetic scheme of starting materials (3) and (6).

2.4. Characterization of N^1-(9,9-diphenyl-9H-fluoren-2-yl)-N^4,N^4-diphenylbenzene-1,4-diamine (3)

Yield: 91%; yellow solid; ^{1}H NMR (500 MHz, $CDCl_3$) δ 9.47–9.49 (d, *J* = 8.0 Hz, 1H), 8.17–8.19 (d, *J* = 8.0 Hz, 1H), 8.09–8.11 (m, 2H), 7.95–8.02 (m, 2H), 7.75–7.89 (m, 2H), 7.59–7.60 (d, *J* = 8.0 Hz, 4H),

7.43–7.44 (d, J = 7.5 Hz, 3H), 7.34–7.36 (d, J = 8.5 Hz, 4H), 7.17–7.19 (d, J = 8.5 Hz, 3H), 6.99–7.02 (t, J = 7.5 Hz, 3H), 6.90–6.93 (t, J = 7.5 Hz, 3H), and 6.39–6.41 (d, J = 8.5 Hz, 3H).

2.5. Synthesis of 2-chloro-4,6-diphenylpyrimidine (**6**)

A mixture of 2,4,6-trichloropyrimidine (4, 0.63 mL, 5.45 mmol), phenylboronic acid (5, 1.39 g, 11.44 mmol), tetrakis(triphenylphosphine)palladium(0) ($Pd(PPh_3P)_4$, 0.18 g, 0.16 mmol), 40 mL of a 2 M aqueous K_2CO_3 solution, 40 mL of water, 25 mL of ethanol, and 80 mL of toluene was added into a two-neck round-bottom flask that was equipped with a condenser, and this mixture was refluxed at 110 °C for 10 h under a nitrogen atmosphere. After the completion of the reaction, the mixture was made up by using dichloromethane (100 mL) and water (80 mL). The organic layer was dried over anhydrous magnesium sulfate and then concentrated. The crude residues were separated by using a silica column and an *n*-hexane:dichloromethane (4:1) solvent system to obtain the intermediate (6) as a white solid (Scheme 1).

2.6. Characterization of 2-chloro-4,6-diphenylpyrimidine (**6**)

Yield: 80%; white solid; ^{1}H NMR (500 MHz, $CDCl_3$) δ 8.13–8.14 (m, 4H), 8.01 (s, 1H), and 7.51–7.55 (m, 6H); ^{13}C NMR (500 MHz, $CDCl_3$) δ 167.7, 162.1, 135.7, 131.7, 129.1, 127.5, and 111.0.

2.7. Synthesis of N^1-(9,9-diphenyl-9H-fluoren-2-yl)-N^1-(4,6-diphenylpyrimidin-2-yl)-N^4,N^4 diphenylbenzene-1,4-diamine (FLU-TPA/PYR)

A mixture of N^1-(9,9-diphenyl-9*H*-fluoren-2-yl)-N^4,N^4-diphenylbenzene-1,4-diamine (3, 1.0 g, 1.73 mmol), 2-chloro-4,6-diphenylpyrimidine (6, 0.50 g, 1.90 mmol), palladium (II) acetate ($Pd(OAc)_2$, 0.08 g, 0.34 mmol), 10% tri-*tert*-butylphosphine in toluene (tBu$_3$P, 0.12 mL, 0.52 mmol), sodium *tert*-butoxide (NaOtBu, 0.28 g, 2.94 mmol), and 80 mL of anhydrous toluene was added into a two-neck round-bottom flask that was equipped with a condenser, and this mixture was refluxed at 110 °C for 12 h in a nitrogen atmosphere while stirring magnetically. The crude residues were separated by a silica column and an *n*-hexane:dichloromethane (1:1) solvent system to obtain the target final product FLU-TPA/PYR, and further purification was carried out using ethyl ether/petroleum ether (Scheme 2).

2.8. Characterization of N^1-(9,9-diphenyl-9H-fluoren-2-yl)-N^1-(4,6-diphenylpyrimidin-2-yl)-N^4,N^4 diphenylbenzene-1,4-diamine (FLU-TPA/PYR)

Yield: 83%; yellow solid; FT-IR (KBr pellet): umax 3056.6, 1586.7, 1562.9, 1536.6, 1505.0, 1491.8, 1452.9, 1403.2, 1353.9, 1306.0, 1272.6, 1234.2, 1184.0, 1155.7, 1108.0, 1070.4, 1029.4, 1001.6, 981.5, 922.7, 883.0, 832.9, and 822.9 cm^{-1}; ^{1}H NMR (500 MHz, $CDCl_3$) δ 7.92–7.93 (d, J = 7.0 Hz, 4H), 7.79–7.81 (d, J = 8.0 Hz, 1H), 7.76–7.77 (d, J = 7.5 Hz, 1H), 7.60 (s, 1H), 7.52 (s, 1H), 7.36–7.45 (m, 9H), 7.25–7.28 (t, J = 8.5 Hz, 5H), 7.19–7.21 (m, 6H), 7.13–7.15 (m, 6H), 7.08–7.11 (m, 6H), 7.00–7.03 (t, J = 7.5 Hz, 2H); ^{13}C NMR (500 MHz, $CDCl_3$) δ 165.2, 162.7, 151.9, 151.3, 147.9, 145.9, 144.7, 144.6, 140.2, 140.0, 137.5, 137.1, 130.6, 129.2, 128.8, 128.2, 127.6, 127.3, 127.1, 126.6, 126.3, 125.5, 124.8, 123.9, 122.6, 120.6, 120.0, and 104.1; MS (APCI) m/z: 806.71 for $C_{59}H_{42}N_4$ [(M + H)$^+$]; Anal. Calcd. for $C_{59}H_{42}N_4$ (%): C, 87.81; H, 5.25; and N, 6.94. Found: C, 88.92; H, 5.33; and N, 7.02.

2.9. Synthesis of N^1-(4-(4,6-diphenyl-1,3,5-triazin-2-yl)phenyl)-N^1-(9,9-diphenyl-9H-fluoren-2-yl)-N^4,N^4-diphenylbenzene-1,4-diamine (FLU-TPA/TRZ)

A mixture of N^1-(9,9-diphenyl-9*H*-fluoren-2-yl)-N^4,N^4-diphenylbenzene-1,4-diamine (3, 1.0 g, 1.73 mmol), 2-(4-bromophenyl)-4,6-diphenyl-1,3,5-triazine (7, 0.74 g, 1.90 mmol), palladium (II) acetate ($Pd(OAc)_2$, 0.08 g, 0.34 mmol), 10% tri-*tert*-butylphosphine in toluene (tBu$_3$P, 0.12 mL, 0.52 mmol), sodium *tert*-butoxide (NaOtBu, 0.28 g, 2.94 mmol) and 80 mL of anhydrous toluene was added into a two-neck round-bottom flask that was equipped with a condenser, and this mixture was refluxed at 110 °C for 12 h in a nitrogen atmosphere while stirring magnetically. The crude residues were

separated by a silica column and an *n*-hexane:dichloromethane (1:1) solvent system to obtain the target final product FLU-TPA/TRZ as a yellow solid (Scheme 2).

2.10. Characterization of N^1-(4-(4,6-diphenyl-1,3,5-triazin-2-yl)phenyl)-N^1-(9,9-diphenyl-9H-fluoren-2-yl)-N^4,N^4-diphenylbenzene-1,4-diamine (FLU-TPA/TRZ)

Yield: 81%; yellow solid; FT-IR (KBr pellet): umax 3034.2, 1587.9, 1523.6, 1505.5, 1489.7, 1444.0, 1427.0, 1410.4, 1366.1, 1308.8, 1281.0, 1266.4, 1183.0, 1147.7, 1109.7, 1077.8, 1026.9, 964.4, 934.6, 892.3, and 828.0 cm^{-1}; ^1H NMR (500 MHz, $CDCl_3$) δ 8.65–8.67 (d, *J* = 7.5 Hz, 4H), 8.50–8.51 (d, *J* = 8.5 Hz, 2H), 7.90–7.91 (d, *J* = 8.0 Hz, 1H), 7.85–7.87 (d, *J* = 7.5 Hz, 1H), 7.59–7.66 (m, 6H), 7.36–7.41 (m, 2H), 7.26–7.30 (m, 5H), 7.20–7.22 (m, 7H), 7.11 (s, 1H), 6.99–7.07 (m, 4H), and 6.93–6.95 (d, *J* = 9.0 Hz, 2H); ^{13}C NMR (500 MHz, $CDCl_3$) δ 147.6, 145.7, 136.1, 133.9, 133.4, 130.1, 129.4, 129.0, 128.9, 128.1, 127.2, 124.2, and 123.5; MS (APCI) *m/z*: 883.63 for $C_{64}H_{45}N_5$ [(M + H)$^+$]; Anal. Calcd. for $C_{64}H_{45}N_5$ (%): C, 86.95; H, 5.13; and N, 7.92. Found: C, 87.62; H, 5.18; and N, 8.01.

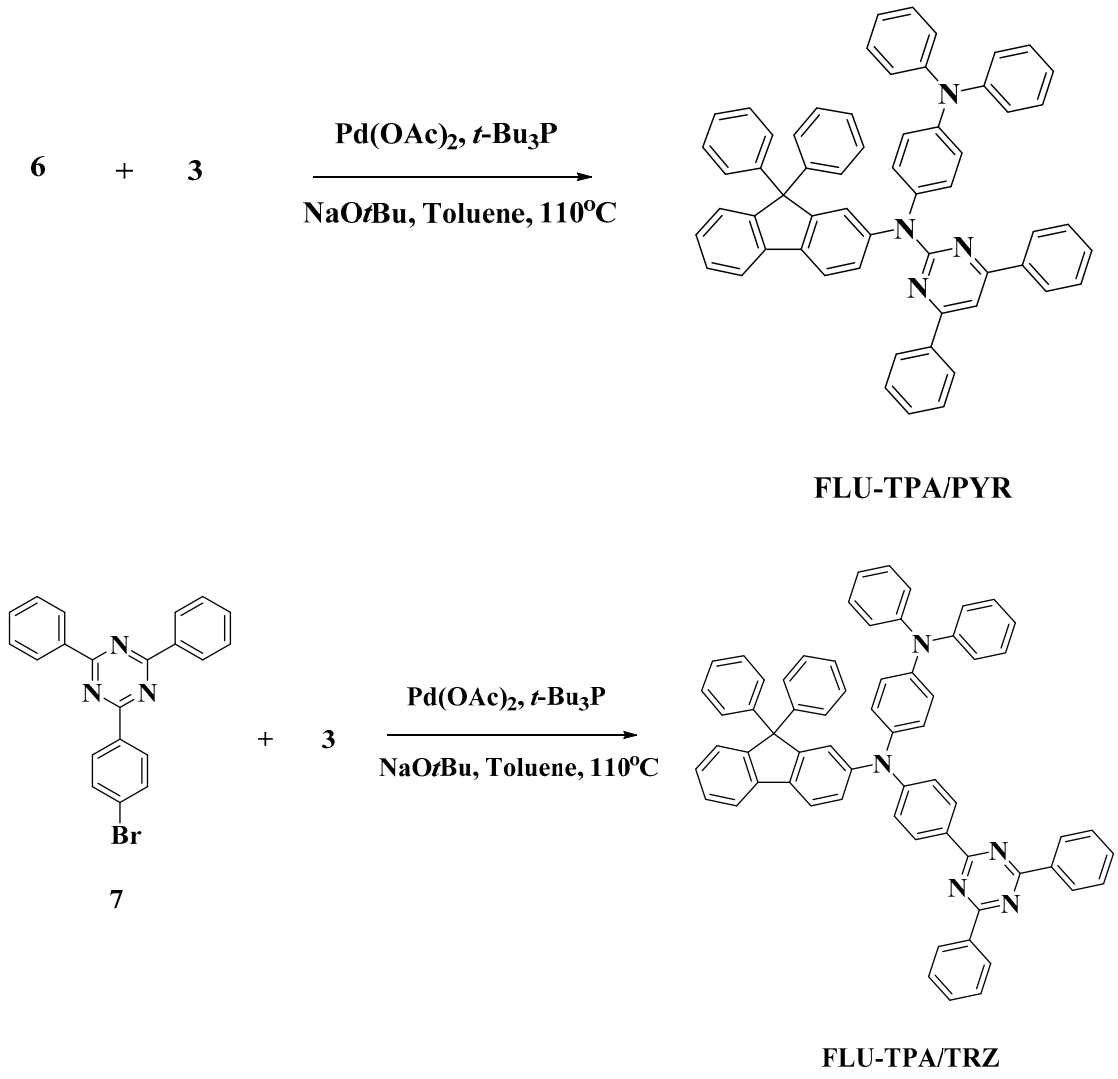

Scheme 2. Synthetic route of target molecules of N^1-(9,9-diphenyl-9*H*-fluoren-2-yl)-N^1-(4,6-diphenylpyrimidin-2-yl)-N^4,N^4-diphenylbenzene-1,4-diamine (FLU-TPA/PYR) and N^1-(4-(4,6-diphenyl-1,3,5-triazin-2-yl)phenyl)-N^1-(9,9-diphenyl-9*H*-fluoren-2-yl)-N^4,N^4 diphenylbenzene-1,4-diamine (FLU-TPA/TRZ).

2.11. OLED Device Fabrication

To construct the OLED devices, indium–tin-oxide (ITO)-coated glass substrates were washed in an ultrasonic bath with isopropyl alcohol and deionized water for 20 min. The cleaned substrates were subjected to a UV–ozone treatment for about 6 min. All the organic layers and the metal cathode were fabricated on the pre-washed ITO-coated glass substrate. The deposition rate of ~5×10^{-7} Torr pressure was applied with a Sunic organic evaporator (Suwon, Korea). All deposition processes were conducted inside a glove box under inert conditions. Each device size area was fabricated as 2 mm^2.

3. Results and Discussions

The thermal properties of FLU-TPA/PYR and FLU-TPA/TRZ were studied with thermal gravimetric analysis (TGA) and differential scanning calorimetry (DSC) under a nitrogen atmosphere. The glass transition temperatures of FLU-TPA/PYR and FLU-TPA/TRZ were 153 and 147 °C, respectively. The thermal decompositions of our FLU-TPA/PYR and FLU-TPA/TRZ were recorded at approximately 426 and 478 °C, respectively, with a 5% weight reduction. Both of our materials exhibited excellent thermal stabilities, which could improve the morphological stabilities during device operation. Thermal properties are shown in Figure 1 and summarized in Table 1.

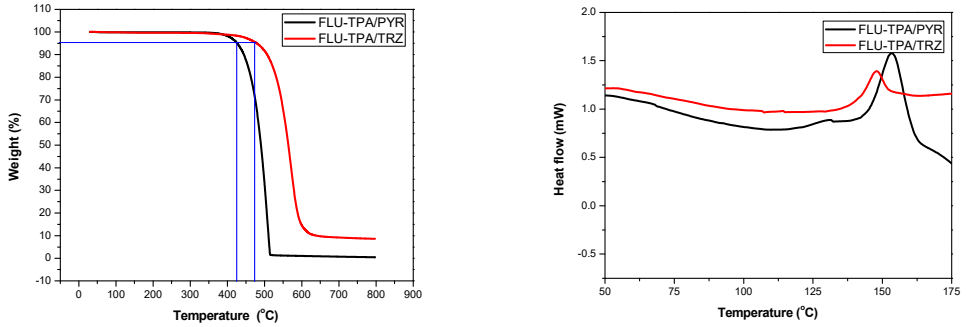

Figure 1. Differential scanning calorimetry (DSC) and thermal gravimetric analysis (TGA) of FLU-TPA/PYR and FLU-TPA/TRZ.

Table 1. Physical properties of FLU-TPA/PYR and FLU-TPA/TRZ.

Bipolar Materials	FLU-TPA/PYR	FLU-TPA/TRZ
T_g (°C)	153	147
T_d (°C)	426	478
UV-Vis (nm)	410	412
PL (nm)	548	606
Band gap (eV)	2.41	2.49
Triplet energy (eV)	2.57	2.77
Highest occupied molecular orbital (HOMO) (eV)	5.27	5.35
Lowest occupied molecular orbital (LUMO) (eV)	2.86	2.86

The UV-Vis absorption and photoluminescent (PL) spectra of FLU-TPA/PYR and FLU-TPA/TRZ are depicted in Figure 2. FLU-TPA/PYR and FLU-TPA/TRZ showed similar absorption at 410 and 412 nm, respectively. The band gap energy values of FLU-TPA/PYR and FLU-TPA/TRZ were recorded at 2.41 and 2.49 eV, and they were associated with onset absorption wavelengths of 515 and 498 nm, respectively. FLU-TPA/PYR showed an extended absorption when compared to FLU-TPA/TRZ. The photoluminescent spectra's maxima were found at 548 and 606 nm, respectively, in the toluene solvent for FLU-TPA/PYR and FLU-TPA/TRZ. Triazine acceptor-based FLU-TPA/TRZ expressed a longer emission peak at room temperature. The triplet energies of FLU-TPA/PYR and FLU-TPA/TRZ were obtained as 2.57 and 2.77 eV, respectively, and this is highly important for a host material to

prevent energy flow back from the dopant material. From this information, we believed that our materials would reveal good efficiency enhancement with yellow phosphorescent OLEDs.

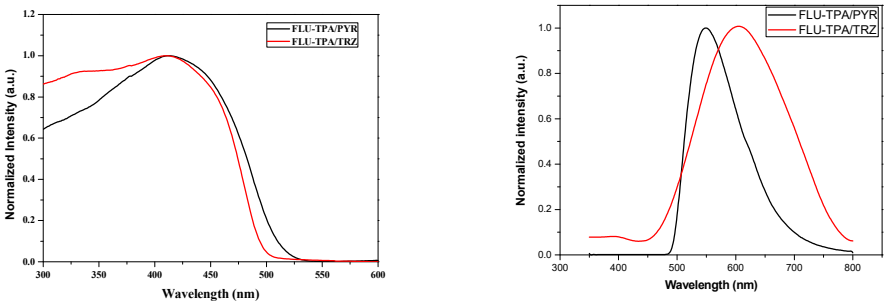

Figure 2. UV-Vis absorption and photoluminescent (PL) spectra of FLU-TPA/PYR and FLU-TPA/TRZ.

The HOMO (highest occupied molecular orbital) energy ere were calculated, and they were found to be −5.27 and 5.35 eV for FLU-TPA/PYR and FLU-TPA/TRZ, respectively. The LUMO (lowest unoccupied molecular orbital) energy values were obtained by adding the bang gap energy to the HOMO energy, and they were −2.86 eV for both FLU-TPA/PYR and FLU-TPA/TRZ. The frontier molecular orbital energies (FMOs) facilitated an effective charge transportation from both the electrodes. To understand the molecular orbital distribution, we used basic density functional theory (DFT) with a basic set of 6–31 G while using a Gaussian 09. The frontier molecular orbital distributions are displayed in Figure 3. The LUMO distribution was noticed over the electron-withdrawing triazine and pyrimidine moieties, while the HOMO distribution was noticed over the electron-donating triphenylamine unit, but the HOMO distribution showed considerable overlapping.

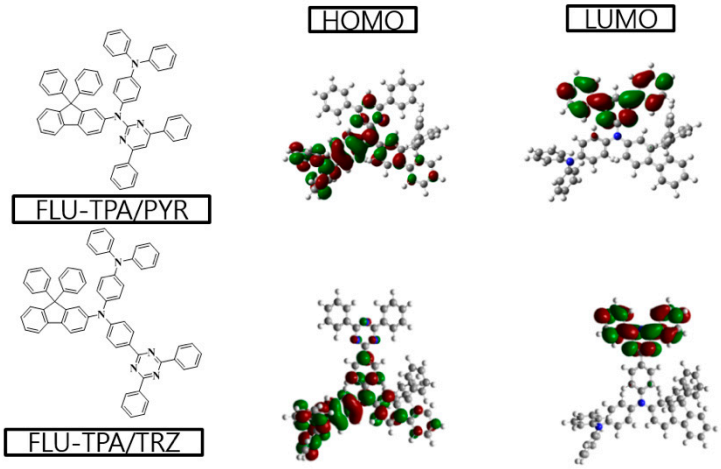

Figure 3. Frontier molecular orbital distributions of FLU-TPA/PYR and FLU-TPA/TRZ.

To establish the electroluminescent properties of our bipolar host materials FLU-TPA/PYR and FLU-TPA/TRZ, yellow phosphorescent OLED devices were fabricated with a PO-O1 yellow dopant (Figure 4). The yellow phosphorescent device structure was as follows: indium–tin oxide (ITO) (150 nm)/1,4,5,8,9,11-hexaazatriphenylenehexacarbonitrile (HATCN) (7 nm)/4,4′-cyclohexylidenebis[N,N-bis(4-methylphenyl)benzenamine](TAPC) (43 nm)/FLU-TPA/PYR or FLU-TPA/TRZ: 10 wt% iridium(III) bis(4-(4-*tert*-butylphenyl) thieno[3,2-c]pyridinato-N,C2′) acetylaceto nate (PO-O1) (20 nm)/1,3,5-tri(m-pyridin-3-ylphenyl)benzene (TmPyPB) (35 nm)/8-quinolinolato lithium (Liq) (1.5 nm)/aluminum (Al) (100 nm). ITO and Al were used for the anode and cathode, respectively, HATCN was used for the hole-injecting layer (HIL), Liq was used for the electron-injecting layer (EIL), TAPC was used as the hole-transporting layer (HTL), and TmPyPB was employed as the electron transport layer (ETL).

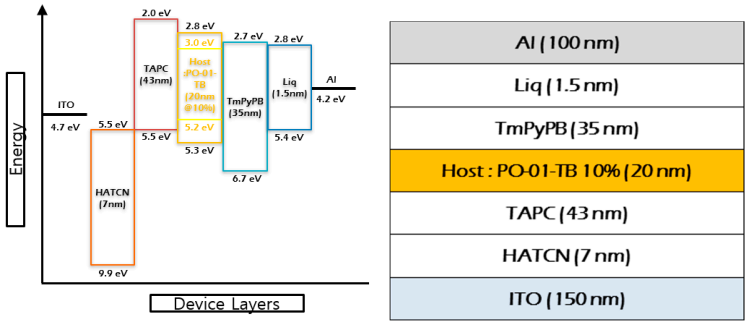

Figure 4. Device structure of yellow phosphorescent organic light-emitting diodes (OLEDs).

The current density–voltage, current density–power, and current efficiencies are depicted in Figure 5 and summarized in Table 2. The turn-on voltage of the FLU-TPA/PYR and FLU-TPA/TRZ-based devices was 5 V. The current efficiencies of the FLU-TPA/PYR and FLU-TPA/TRZ-based devices were 21.70 and 18.72 cd/A, respectively. Consequently, the power efficiencies was observed as 13.64 and 11.76 lm/W for FLU-TPA/PYR and FLU-TPA/TRZ, respectively. The external quantum efficiency (7.75%) of the FLU-TPA/PYR-based device was higher than that of the triazine-based FLU-TPA/TRZ device (6.44%). Though both devices exhibited a similar turn-on voltage, the device efficiencies of the pyrimidine-based FLU-TPA/PYR were considerably higher than those of FLU-TPA/TRZ. Both the devices showed lower efficiency roll-off, which is one of the important factors for longer operation devices. The electro luminescent (EL) spectra of both devices are depicted in Figure 6. The maximum emission of both yellow devices was similar at 562 nm, which substantiated the yellow emission from the yellow dopant.

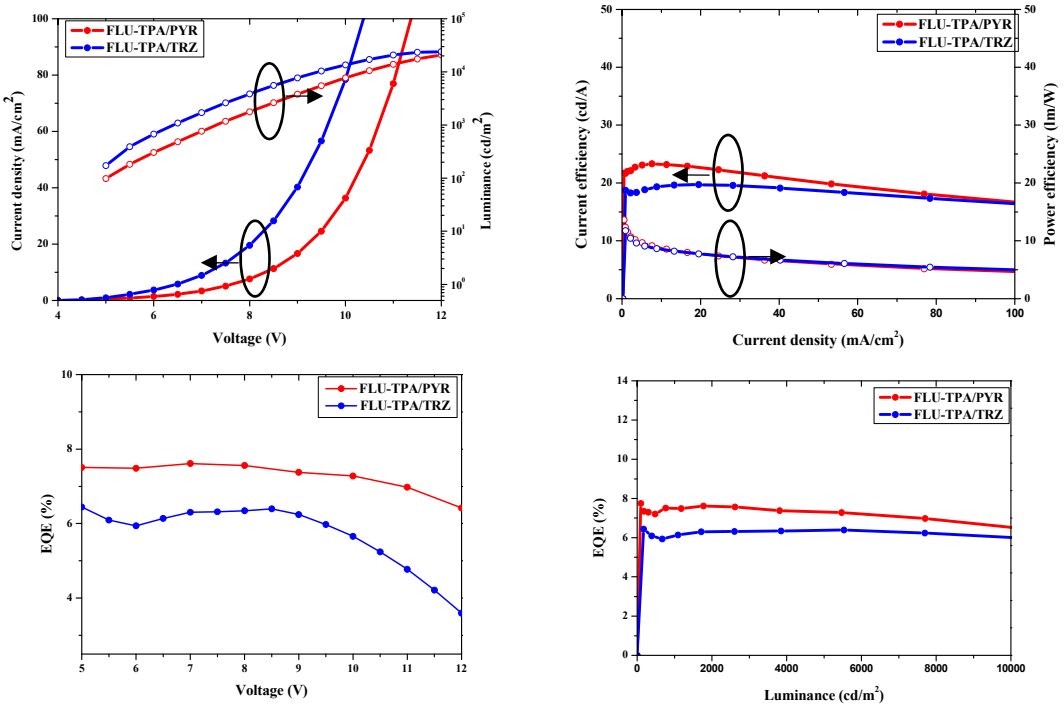

Figure 5. Current density–voltage, luminescence–voltage, and external quantum efficiencies of yellow phosphorescent OLEDs.

Table 2. Device characteristics of FLU-TPA/PYR and FLU-TPA/TRZ-based phosphorescent and non-doped fluorescent devices.

Device Characteristics	FLU-TPA/PYR (Yellow Device)	FLU-TPA/TRZ (Yellow Device)	FLU-TPA/PYR (Non-Doped)	FLU-TPA/TRZ (Non-Doped)
Turn-On Voltage (V)	5.0	5.0	6.5	5.0
Current Efficiency (cd/A)	21.70	18.72	1.27	10.30
Power Efficiency (lm/W)	13.64	11.76	0.61	6.47
EQE (%)	7.75	6.44	0.53	3.57
CIE (x,y)	0.49,0.50	0.49,0.50	0.41,0.51	0.41,0.55

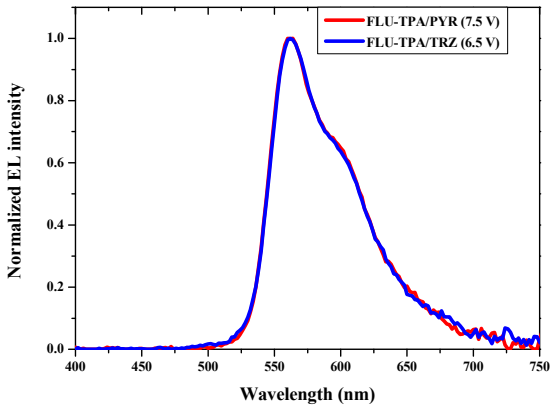

Figure 6. Electroluminescent spectra of yellow phosphorescent OLEDs.

Moreover, we fabricated non-doped fluorescence devices to understand the performances of our molecules as emitters (Figure 7). The non-doped device structure was as follows: indium–tin oxide (ITO) (150 nm)/1,4,5,8,9,11-hexaazatriphenylenehexacarbonitrile (HATCN) (7 nm)/4,4′-cyclohexylidenebis[*N*,*N*-bis(4-methylphenyl)benzenamine](TAPC) (43 nm)/FLU-TPA/PYR or FLU-TPA/TRZ (20 nm)/1,3,5-tri(m-pyridin-3-ylphenyl)benzene (TmPyPB) (35 nm)/8-quinolinolato lithium (Liq) (1.5 nm)/aluminum (Al) (100 nm).

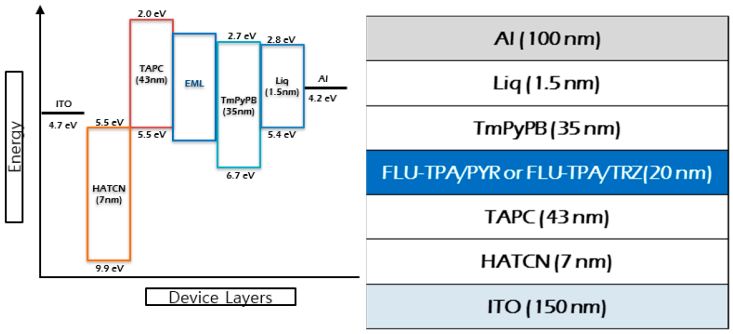

Figure 7. Device structure of non-doped fluorescent OLEDs.

The non-doped device performances of the triazine-based FLU-TPA/TRZ was much better than that of the pyridine-based FLU-TPA/PYR. The current, power and external quantum efficiencies of the FLU-TPA/TRZ-based device were 10.30 cd/A, 6.47 lm/W and 3.57%, respectively (Figure 8 and Table 2). The maximum EL emission was observed at 549 nm, which was related to the CIE color coordinates (x, y) of 0.41, 0.55 with the emission of green color (Figure 9).

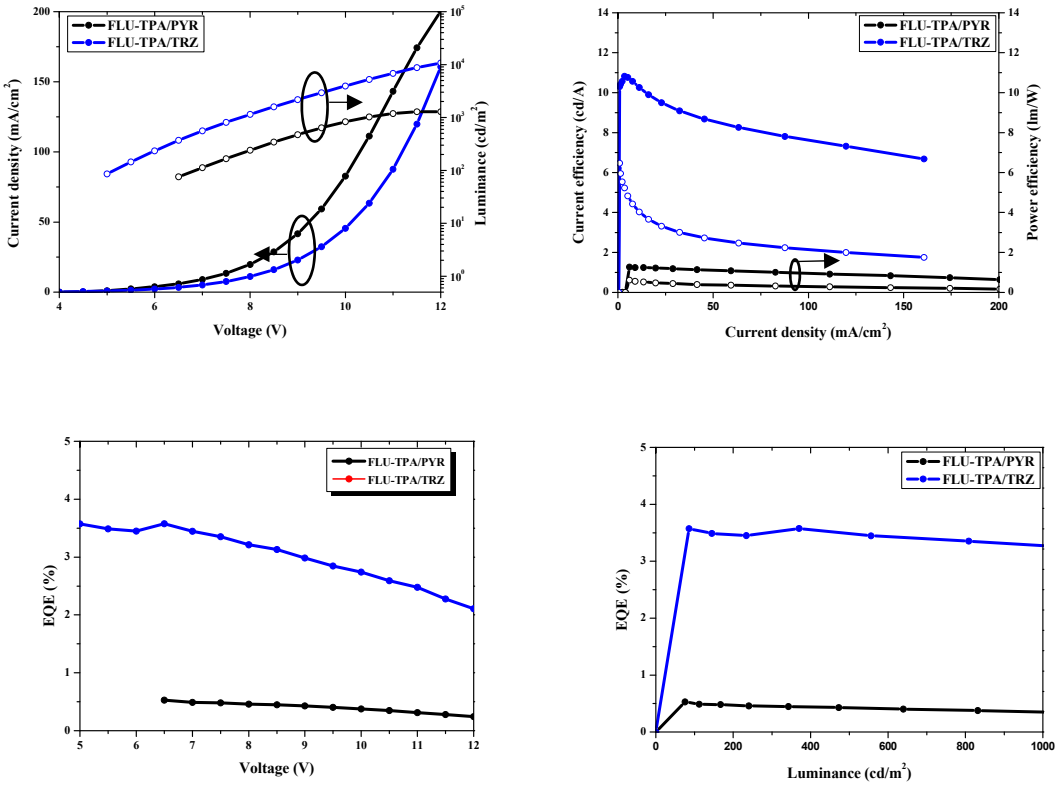

Figure 8. Current density–voltage, luminescence–voltage, and external quantum efficiencies of non-doped fluorescent OLEDs.

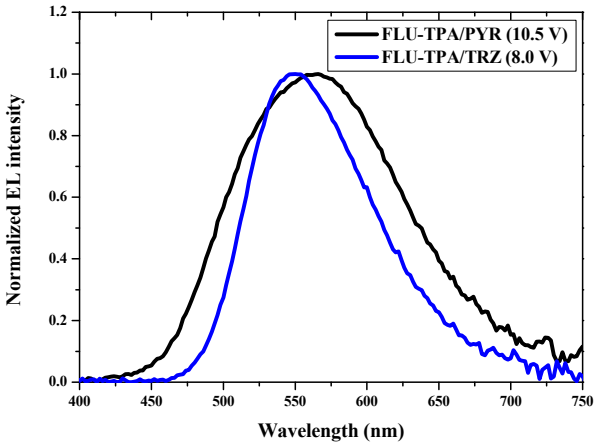

Figure 9. Electroluminescent spectra of non-doped fluorescent OLEDs.

4. Conclusions

Two bipolar materials were synthesized with an N^1-(9,9-diphenyl-9*H*-fluoren-2-yl)-N^4,N^4-dipheny lbenzene-1,4-diamine donor and a triazine or pyrimidine acceptor. The bipolar materials FLU-TPA/PYR and FLU-TPA/TRZ were applied in yellow phosphorescent and non-doped fluorescent OLEDs. The yellow device with FLU-TPA/PYR showed good device characteristics when compared to the triazine-based FLU-TPA/TRZ. The current and power efficiencies of the FLU-TPA/PYR-based yellow device were measured at 21.70 cd/A and 13.64 lm/W, respectively. However, the FLU-TPA/TRZ-based non-doped fluorescent device revealed excellent device properties compared to the pyrimidine-based FLU-TPA/PYR. All devices exhibited a lower efficiency roll-off, and our new molecular design will be helpful to develop thermally stable host materials in the future.

Author Contributions: Conceptualization, R.B. and K.Y.C.; methodology, R.B. and B.M.K.; software, R.B.; formal analysis, I.-J.B. and R.B.; resources, K.Y.C.; material synthesis, H.J. and K.K.; writing—original draft preparation, R.B.; writing—review and editing, R.B.; supervision, K.Y.C. and M.K.; project administration, K.Y.C.; funding acquisition, K.Y.C. All authors have read and agreed to the published version of the manuscript.

Funding: This research was supported by the Basic Science Research Program through the National Research Foundation of Korea (NRF), funded by the education grant NRF-2016R1D1A3B01015531.

Conflicts of Interest: The authors declare no conflict of interest.

References

1. Ito, T.; Sasabe, H.; Nagai, Y.; Watanabe, Y.; Onuma, N.; Kido, J. A series of dibenzofuran-based n-type exciplex host partners realizing high-efficiency and stable deep-red phosphorescent oleds. *Chem. A Eur. J.* **2019**, *25*, 7308–7314. [CrossRef]
2. Kido, J.; Kimura, M.; Nagai, K. Multilayer white light-emitting organic electroluminescent device. *Science* **1995**, *267*, 1332–1334. [CrossRef]
3. Braveenth, R.; Bae, H.W.; Ko, I.J.; Qiong, W.; Nguyen, Q.P.B.; Jayashantha, P.G.S.; Kwon, J.H.; Chai, K.Y. Thermally stable efficient hole transporting materials based on carbazole and triphenylamine core for red phosphorescent oleds. *Org. Electron.* **2017**, *51*, 463–470. [CrossRef]
4. Promarak, V.; Ichikawa, M.; Meunmart, D.; Sudyoadsuk, T.; Saengsuwan, S.; Keawin, T. Synthesis and properties of stable amorphous hole-transporting molecules for electroluminescent devices. *Tetrahedron Lett.* **2006**, *47*, 8949–8952. [CrossRef]
5. Kim, B.M.; Nguyen, Q.P.B.; Fan, J.G.; Kim, M.J.; Braveenth, R.; Kim, G.W.; Kwon, J.H.; Chai, K.Y. Novel star-shaped hole-transporting materials based on triphenylamine cores end-capped with carbazole and triarylamine derivatives for use in oleds. *Bull. Korean Chem. Soc.* **2015**, *36*, 1303–1306. [CrossRef]
6. Kochapradist, P.; Prachumrak, N.; Tarsang, R.; Keawin, T.; Jungsuttiwong, S.; Sudyoadsuk, T.; Promarak, V. Multi-triphenylamine-substituted carbazoles: Synthesis, characterization, properties and applications as hole-transporting materials. *Tetrahedron Lett.* **2013**, *54*, 3683–3687. [CrossRef]
7. Lee, J.-H.; Chen, C.-H.; Lee, P.-H.; Lin, H.-Y.; Leung, M.-k.; Chiu, T.-L.; Lin, C.-F. Blue organic light-emitting diodes: Current status, challenges, and future outlook. *J. Mater. Chem. C* **2019**, *7*, 5874–5888. [CrossRef]
8. Xiao, P.; Dong, T.; Xie, J.; Luo, D.; Yuan, J.; Liu, B. Emergence of white organic light-emitting diodes based on thermally activated delayed fluorescence. *Appl. Sci.* **2018**, *8*, 299. [CrossRef]
9. Braveenth, R.; Chai, K.Y. Triazine-acceptor-based green thermally activated delayed fluorescence materials for organic light-emitting diodes. *Materials* **2019**, *12*, 2646. [CrossRef]
10. Yu, H.; Dai, X.; Yao, F.; Wei, X.; Cao, J.; Jhun, C. Efficient white phosphorescent organic light-emitting diodes using ultrathin emissive layers (<1 nm). *Sci. Rep.* **2018**, *8*, 6068.
11. Kaji, H.; Suzuki, H.; Fukushima, T.; Shizu, K.; Suzuki, K.; Kubo, S.; Komino, T.; Oiwa, H.; Suzuki, F.; Wakamiya, A.; et al. Purely organic electroluminescent material realizing 100% conversion from electricity to light. *Nat. Commun.* **2015**, *6*, 8476. [CrossRef] [PubMed]
12. D'Andrade, B. 5—Phosphorescent oleds for solid-state lighting. In *Organic Light-Emitting Diodes (Oleds)*; Buckley, A., Ed.; Woodhead Publishing: Cambridge, UK, 2013; pp. 143–169.
13. Chen, J.-X.; Tao, W.-W.; Xiao, Y.-F.; Tian, S.; Chen, W.-C.; Wang, K.; Yu, J.; Geng, F.-X.; Zhang, X.-H.; Lee, C.-S. Isomeric thermally activated delayed fluorescence emitters based on indolo[2,3-*b*]acridine electron-donor: A compromising optimization for efficient orange–red organic light-emitting diodes. *J. Mater. Chem. C* **2019**, *7*, 2898–2904. [CrossRef]
14. Fukagawa, H.; Shimizu, T.; Kamada, T.; Kiribayashi, Y.; Osada, Y.; Hasegawa, M.; Morii, K.; Yamamoto, T. Highly efficient and stable phosphorescent organic light-emitting diodes utilizing reverse intersystem crossing of the host material. *Adv. Opt. Mater.* **2014**, *2*, 1070–1075. [CrossRef]
15. Zhan, G.; Liu, Z.; Bian, Z.; Huang, C. Recent advances in organic light-emitting diodes based on pure organic room temperature phosphorescence materials. *Front. Chem.* **2019**, *7*, 305. [CrossRef]
16. Wagner, D.; Hoffmann, S.T.; Heinemeyer, U.; Münster, I.; Köhler, A.; Strohriegl, P. Triazine based bipolar host materials for blue phosphorescent oleds. *Chem. Mater.* **2013**, *25*, 3758–3765. [CrossRef]

17. Cui, L.-S.; Kim, J.U.; Nomura, H.; Nakanotani, H.; Adachi, C. Benzimidazobenzothiazole-based bipolar hosts to harvest nearly all of the excitons from blue delayed fluorescence and phosphorescent organic light-emitting diodes. *Angew. Chem. Int. Ed.* **2016**, *55*, 6864–6868. [CrossRef]
18. Mori, K.; Goumans, T.P.M.; van Lenthe, E.; Wang, F. Predicting phosphorescent lifetimes and zero-field splitting of organometallic complexes with time-dependent density functional theory including spin–orbit coupling. *Phys. Chem. Chem. Phys.* **2014**, *16*, 14523–14530. [CrossRef]
19. Chou, P.-T.; Chi, Y. Osmium- and ruthenium-based phosphorescent materials: Design, photophysics and utilization in oled fabrication. *Eur. J. Inorg. Chem.* **2006**, *2006*, 3319–3332. [CrossRef]
20. Wong, W.-Y.; Ho, C.-L. Heavy metal organometallic electrophosphors derived from multi-component chromophores. *Coord. Chem. Rev.* **2009**, *253*, 1709–1758. [CrossRef]
21. Kawamura, Y.; Goushi, K.; Brooks, J.; Brown, J.J.; Sasabe, H.; Adachi, C. 100% phosphorescence quantum efficiency of ir(iii) complexes in organic semiconductor films. *Appl. Phys. Lett.* **2005**, *86*, 071104. [CrossRef]
22. Shih, P.-I.; Chiang, C.-L.; Dixit, A.K.; Chen, C.-K.; Yuan, M.-C.; Lee, R.-Y.; Chen, C.-T.; Diau, E.W.-G.; Shu, C.-F. Novel carbazole/fluorene hybrids: Host materials for blue phosphorescent oleds. *Org. Lett.* **2006**, *8*, 2799–2802. [CrossRef] [PubMed]
23. Gong, X.; Robinson, M.R.; Ostrowski, J.C.; Moses, D.; Bazan, G.C.; Heeger, A.J. High-efficiency polymer-based electrophosphorescent devices. *Adv. Mater.* **2002**, *14*, 581–585. [CrossRef]
24. Jiang, Z.; Chen, Y.; Yang, C.; Cao, Y.; Tao, Y.; Qin, J.; Ma, D. A fully diarylmethylene-bridged triphenylamine derivative as novel host for highly efficient green phosphorescent oleds. *Org. Lett.* **2009**, *11*, 1503–1506. [CrossRef] [PubMed]
25. Liu, D.; Sun, K.; Zhao, G.; Wei, J.; Duan, J.; Xia, M.; Jiang, W.; Sun, Y. Spatial separation of a tadf sensitizer and fluorescent emitter with a core-dendron system to block the energy loss in deep blue organic light-emitting diodes. *J. Mater. Chem. C* **2019**, *7*, 11005–11013. [CrossRef]
26. Song, D.; Zhao, S.; Luo, Y.; Aziz, H. Causes of efficiency roll-off in phosphorescent organic light emitting devices: Triplet-triplet annihilation versus triplet-polaron quenching. *Appl. Phys. Lett.* **2010**, *97*, 243304. [CrossRef]
27. Serevičius, T.; Komskis, R.; Adomėnas, P.; Adomėnienė, O.; Kreiza, G.; Jankauskas, V.; Kazlauskas, K.; Miasojedovas, A.N.; Jankus, V.; Monkman, A.; et al. Triplet–triplet annihilation in 9, 10-diphenylanthracene derivatives: The role of intersystem crossing and exciton diffusion. *J. Phys. Chem. C* **2017**, *121*, 8515–8524. [CrossRef]
28. Flügge, H.; Rohr, A.; Döring, S.; Fléchon, C.; Wallesch, M.; Zink, D.; Seeser, J.; Leganés, J.; Sauer, T.; Rabe, T.; et al. *Reduced Concentration Quenching in a Tadf-Type Copper(I)-Emitter*; SPIE: Bellingham, WA, USA, 2015; Volume 9566.
29. Wang, Z.; Li, M.; Gan, L.; Cai, X.; Li, B.; Chen, D.; Su, S.-J. Predicting operational stability for organic light-emitting diodes with exciplex cohosts. *Adv. Sci.* **2019**, *6*, 1802246. [CrossRef]
30. Huang, R.; Kukhta, N.A.; Ward, J.S.; Danos, A.; Batsanov, A.S.; Bryce, M.R.; Dias, F.B. Balancing charge-transfer strength and triplet states for deep-blue thermally activated delayed fluorescence with an unconventional electron rich dibenzothiophene acceptor. *J. Mater. Chem. C* **2019**, *7*, 13224–13234. [CrossRef]
31. Shakeel, U.; Singh, J. Study of processes of reverse intersystem crossing (RISC) and thermally activated delayed fluorescence (TADF) in organic light emitting diodes (OLEDS). *Org. Electron.* **2018**, *59*, 121–124. [CrossRef]
32. Zhao, C.; Li, C.; Li, Y.; Qiu, Y.; Duan, L. Understanding the operational lifetime expansion methods of thermally activated delayed fluorescence sensitized oleds: A combined study of charge trapping and exciton dynamics. *Mater. Chem. Front.* **2019**, *3*, 1181–1191. [CrossRef]
33. Hosokai, T.; Matsuzaki, H.; Nakanotani, H.; Tokumaru, K.; Tsutsui, T.; Furube, A.; Nasu, K.; Nomura, H.; Yahiro, M.; Adachi, C. Evidence and mechanism of efficient thermally activated delayed fluorescence promoted by delocalized excited states. *Sci. Adv.* **2017**, *3*, e1603282. [CrossRef] [PubMed]
34. Chen, J.-X.; Tao, W.-W.; Wang, K.; Zheng, C.-J.; Liu, W.; Li, X.; Ou, X.-M.; Zhang, X.-H. Highly efficient thermally activated delayed fluorescence emitters based on novel indolo[2,3-*b*]acridine electron-donor. *Org. Electron.* **2018**, *57*, 327–334. [CrossRef]
35. dos Santos, P.L.; Ward, J.S.; Bryce, M.R.; Monkman, A.P. Using guest–host interactions to optimize the efficiency of tadf oleds. *J. Phys. Chem. Lett.* **2016**, *7*, 3341–3346. [CrossRef] [PubMed]

36. Jeon, W.S.; Park, T.J.; Kim, S.Y.; Pode, R.; Jang, J.; Kwon, J.H. Ideal host and guest system in phosphorescent oleds. *Org. Electron.* **2009**, *10*, 240–246. [CrossRef]
37. Lee, H.L.; Lee, K.H.; Lee, J.Y. Indoloindole as a new building block of a hole transport type host for stable operation in phosphorescent organic light-emitting diodes. *J. Mater. Chem. C* **2019**, *7*, 5988–5994. [CrossRef]
38. Jung, M.; Lee, J.Y. Exciplex hosts for blue phosphorescent organic light-emitting diodes. *J. Inf. Disp.* **2019**, 1–8. [CrossRef]
39. Lee, S.; Koo, H.; Kwon, O.; Jae Park, Y.; Choi, H.; Lee, K.; Ahn, B.; Min Park, Y. The role of charge balance and excited state levels on device performance of exciplex-based phosphorescent organic light emitting diodes. *Sci. Rep.* **2017**, *7*, 11995. [CrossRef]
40. Cheng, T.-Y.; Lee, J.-H.; Chen, C.-H.; Chen, P.-H.; Wang, P.-S.; Lin, C.-E.; Lin, B.-Y.; Lan, Y.-H.; Hsieh, Y.-H.; Huang, J.-J.; et al. Carrier transport and recombination mechanism in blue phosphorescent organic light-emitting diode with hosts consisting of cabazole- and triazole-moiety. *Sci. Rep.* **2019**, *9*, 3654. [CrossRef]
41. Lin, M.-S.; Yang, S.-J.; Chang, H.-W.; Huang, Y.-H.; Tsai, Y.-T.; Wu, C.-C.; Chou, S.-H.; Mondal, E.; Wong, K.-T. Incorporation of a cn group into mcp: A new bipolar host material for highly efficient blue and white electrophosphorescent devices. *J. Mater. Chem.* **2012**, *22*, 16114–16120. [CrossRef]
42. Kang, J.S.; Hong, T.R.; Kim, H.J.; Son, Y.H.; Lampande, R.; Kang, B.Y.; Lee, C.; Bin, J.-K.; Lee, B.S.; Yang, J.H.; et al. High-performance bipolar host materials for blue tadf devices with excellent external quantum efficiencies. *J. Mater. Chem. C* **2016**, *4*, 4512–4520. [CrossRef]
43. Zhang, T.; Liang, Y.; Cheng, J.; Li, J. A cbp derivative as bipolar host for performance enhancement in phosphorescent organic light-emitting diodes. *J. Mater. Chem. C* **2013**, *1*, 757–764. [CrossRef]
44. Maasoumi, F.; Jansen-van Vuuren, R.D.; Shaw, P.E.; Puttock, E.V.; Nagiri, R.C.R.; McEwan, J.A.; Bown, M.; O'Connell, J.L.; Dunn, C.J.; Burn, P.L.; et al. An external quantum efficiency of >20% from solution-processed poly(dendrimer) organic light-emitting diodes. *Npj Flex. Electron.* **2018**, *2*, 27. [CrossRef]
45. Zhang, B.; Xie, Z. Recent applications of interfacial exciplex as ideal host of power-efficient oleds. *Front. Chem.* **2019**, *7*, 306. [CrossRef] [PubMed]
46. Lin, T.; Sun, X.; Hu, Y.; Mu, W.; Sun, Y.; Zhang, D.; Su, Z.; Chu, B.; Cui, Z. Blended host ink for solution processing high performance phosphorescent oleds. *Sci. Rep.* **2019**, *9*, 6845. [CrossRef] [PubMed]
47. Kang, G.W.; Lee, C. Effect of host materials on eelectrophosphorescence properties of ptoep-doped organic light-emitting diodes. *J. Inf. Disp.* **2007**, *8*, 15–19. [CrossRef]
48. Ihn, S.-G.; Lee, N.; Jeon, S.O.; Sim, M.; Kang, H.; Jung, Y.; Huh, D.H.; Son, Y.M.; Lee, S.Y.; Numata, M.; et al. An alternative host material for long-lifespan blue organic light-emitting diodes using thermally activated delayed fluorescence. *Adv. Sci.* **2017**, *4*, 1600502. [CrossRef]
49. Kim, G.W.; Bae, H.W.; Lampande, R.; Ko, I.J.; Park, J.H.; Lee, C.Y.; Kwon, J.H. Highly efficient single-stack hybrid cool white oled utilizing blue thermally activated delayed fluorescent and yellow phosphorescent emitters. *Sci. Rep.* **2018**, *8*, 16263. [CrossRef]
50. Braveenth, R.; Ahn, D.H.; Han, J.-H.; Moon, J.S.; Kim, S.W.; Lee, H.; Qiong, W.; Kwon, J.H.; Chai, K.Y. Utilizing triazine/pyrimidine acceptor and carbazole-triphenylamine donor based bipolar novel host materials for highly luminescent green phosphorescent oleds with lower efficiency roll-off. *Dye. Pigment.* **2018**, *157*, 377–384. [CrossRef]
51. Lee, D.R.; Lee, C.W.; Lee, J.Y. High triplet energy host materials for blue phosphorescent organic light-emitting diodes derived from carbazole modified orthophenylene. *J. Mater. Chem. C* **2014**, *2*, 7256–7263. [CrossRef]
52. Godumala, M.; Choi, S.; Kim, S.K.; Kim, S.W.; Kwon, J.H.; Cho, M.J.; Choi, D.H. Highly efficient bipolar host materials towards solution-processable blue and green thermally activated delayed fluorescence organic light emitting diodes. *J. Mater. Chem. C* **2018**, *6*, 10000–10009. [CrossRef]
53. Feng, Z.; Gao, Z.; Qu, W.; Yang, T.; Li, J.; Wang, L. Rational design of quinoxaline-based bipolar host materials for highly efficient red phosphorescent organic light-emitting diodes. *Rsc Adv.* **2019**, *9*, 10789–10795. [CrossRef]
54. Cha, J.-R.; Lee, C.W.; Gong, M.-S. Bipolar host material for phosphorescent oleds based on 2, 7-diazacarbazole as a new electron-transporting unit. *Bull. Korean Chem. Soc.* **2017**, *38*, 1016–1022. [CrossRef]
55. Vadagaonkar, K.S.; Yang, C.-J.; Zeng, W.-H.; Chen, J.-H.; Patil, B.N.; Chetti, P.; Chen, L.-Y.; Chaskar, A.C. Triazolopyridine hybrids as bipolar host materials for green phosphorescent organic light-emitting diodes (oleds). *Dyes Pigment.* **2019**, *160*, 301–314. [CrossRef]

56. Chang, C.-H.; Kuo, M.-C.; Lin, W.-C.; Chen, Y.-T.; Wong, K.-T.; Chou, S.-H.; Mondal, E.; Kwong, R.C.; Xia, S.; Nakagawa, T.; et al. A dicarbazole–triazine hybrid bipolar host material for highly efficient green phosphorescent oleds. *J. Mater. Chem.* **2012**, *22*, 3832–3838. [CrossRef]
57. Li, W.; Li, J.; Liu, D.; Wang, F.; Zhang, S. Bipolar host materials for high-efficiency blue phosphorescent and delayed-fluorescence oleds. *J. Mater. Chem. C* **2015**, *3*, 12529–12538. [CrossRef]